Eur. Phys. J. D **5**, 119–134 (1999)

THE EUROPEAN PHYSICAL JOURNAL D

EDP Sciences

Floquet theory for short laser pulses

K. Drese[a] and M. Holthaus[b]

Fachbereich Physik der Philipps-Universität, Renthof 6, 35032 Marburg, Germany

Received: 23 June 1998 / Revised: 18 August 1998 / Accepted: 25 August 1998

Abstract. We develop adiabatic perturbation theory for quantum systems responding to short laser pulses, with or without a frequency chirp. Our approach rests on lifting the time-dependent Schrödinger equation to an extended Hilbert space, then applying standard perturbational techniques to Floquet states in this extended space, and finally projecting back to the physical Hilbert space. The same strategy also allows us to construct superadiabatic bases for monitoring the quantum evolution in the course of a pulse. These bases provide a diagnostic tool for improving the efficiency of pulse-induced population transfer. The formalism is applied to the selective excitation of molecular vibrational states by chirped laser pulses, which exploit either successive single-photon resonances or a multiphoton resonance, and by a STIRAP-like process.

PACS. 42.50.Hz Strong-field excitation of optical transitions in quantum systems; multi-photon processes; dynamic Stark shift – 32.80.Bx Level crossing and optical pumping – 03.65.-w Quantum mechanics

1 Introduction

Laser pulses with well-controlled temporal characteristics of amplitude and frequency have a high potential for selective manipulation of the internal state of atoms and molecules [1]. The theoretical analysis of such processes is quite demanding, since it requires the solution of the time-dependent Schrödinger equation for systems with several variable or adjustable parameters. Provided the pulse's envelope and frequency do not vary too rapidly, adiabatic techniques are of great value. However, an adiabatic analysis should be accompanied by the description of non-adiabatic processes that occur inevitably when the pulses are short.

In the present paper we develop such an adiabatic description of laser-pulsed N-level systems, based on the adiabatic response of Floquet states. We start in Section 2 by formulating the adiabatic principle for Floquet states, in a manner that is particularly useful when the laser frequency is chirped. This yields the necessary prerequisites for Section 3, where we quantify the deviations from the ideal adiabatic behavior by elaborating and testing adiabatic perturbation theory for Floquet states, and the Landau-Zener description of multiphoton transitions among Floquet states. An appealing way of investigating quantum evolution beyond the adiabatic limit, relying on the use of superadiabatic bases, is adapted to the Floquet picture in Section 4. After these theoretical developments, we compare in Section 5 two mechanisms for the selective excitation of molecular vibrational states: a sequential chirp around successive single-photon resonances, and a multiphoton chirp. In Section 6 we show how STIRAP-like population transfer schemes fit into our framework. Finally, we discuss our results in Section 7.

[a] e-mail: drese@stat.physik.uni-marburg.de
[b] e-mail: holthaus@stat.physik.uni-marburg.de

2 Adiabatic response of Floquet states

We consider an N-level quantum system, described by a Hamiltonian matrix H_0 with eigenstates $|n\rangle$ ($n=1, \ldots, N$), which interacts with a classical radiation pulse. The total Hamiltonian then is of the form

$$H(t) = H_0 + \widehat{\mu} F(t) \sin(\phi(t)), \tag{1}$$

where $\widehat{\mu}$ is the dipole matrix, $F(t)$ describes the envelope of the pulse's electric field, and the phase $\phi(t)$ is a strictly monotonically increasing, smooth function of time. Its derivative,

$$\frac{d\phi(t)}{dt} \equiv \omega(t), \tag{2}$$

is the instantaneous radiation frequency. We assume that the time interval during which ω changes significantly is large compared to the instantaneous oscillation period $T = 2\pi/\omega$, as is the case for conventionally chirped laser pulses. Likewise, it is understood that during the entire pulse the envelope $F(t)$ varies only slightly and smoothly on the time scale set by T.

We wish to understand, from an analytical point of view, the principles that determine the response of the system H_0 to the pulse. Given some initial state $|\psi(t_i)\rangle$, usually an eigenstate of H_0, and assuming that the pulse

is fired in the time interval between t_i and t_f, we have to solve the time-dependent Schrödinger equation

$$i\hbar\frac{d}{dt}|\psi(t)\rangle = H(t)|\psi(t)\rangle \tag{3}$$

for $t_i \le t \le t_f$, and explain the distribution of the final wave function $|\psi(t_f)\rangle$ over the H_0-eigenstates. The goal is to extract guidelines for robust, selective population transfer from the initial state to a certain prescribed target state, to identify obstacles that might prohibit an efficient transfer, and, if possible, to develop strategies for overcoming them.

Although this problem is too wide in scope to be solved in full generality, even in cases where H_0 comprises just two or three levels, it is certainly possible to pin down its most decisive features. This is due to the fact that the Hamiltonian (1) becomes strictly periodic in time if both F and ω are kept fixed at any value that is met during the pulse. Each $T(\omega)$-periodic Hamiltonian obtained in this way has a complete set of Floquet states [2,3], and the adiabatic theorem of quantum mechanics allows us to relate the solution of the Schrödinger equation (3) to these states [4–7], at least if the parameters vary sufficiently slowly. Utilizing the adiabatic principle for developing optimal pulse strategies then requires to find out what "sufficiently slowly" means in practice, and to control, or deliberately exploit, deviations from the rigidly adiabatic evolution.

2.1 Instantaneous Floquet states

For carrying through this program in detail, we first switch from the physical time t to the dimensionless phase ϕ as the independent variable. This is always possible, since $\phi(t)$ is strictly monotonically increasing; ϕ will play the role of a rescaled time in the following. Writing $F(\phi)$, $\omega(\phi)$ and $|\psi(\phi)\rangle$ instead of $F(t(\phi))$, $\omega(t(\phi))$ and $|\psi(t(\phi))\rangle$, the Schrödinger equation becomes

$$i\hbar\omega(\phi)\frac{d}{d\phi}|\psi(\phi)\rangle = \left(H_0 + \widehat{\mu}F(\phi)\sin(\phi)\right)|\psi(\phi)\rangle. \tag{4}$$

Next, we collect the pulse parameters in a formal vector $R \equiv (F,\omega)$. Keeping R *fixed*, instead of considering pulses $R(\phi)$, each particular choice of R then yields an instantaneous scaled Hamiltonian

$$K^R(\phi) \equiv (\hbar\omega)^{-1}\left(H_0 + \widehat{\mu}F\sin(\phi)\right), \tag{5}$$

which satisfies

$$K^R(\phi) = K^R(\phi + 2\pi). \tag{6}$$

As a consequence of going from t to ϕ, the scaled Hamiltonian is always 2π-periodic, whereas the instantaneous period of the original Hamiltonian (1) varies when the frequency is chirped.

The Floquet theorem now provides [2,3] for each fixed R a set of *Floquet states* $|\psi_\alpha^R(\phi)\rangle$,

$$|\psi_\alpha^R(\phi)\rangle = |u_\alpha^R(\phi)\rangle \exp\left(-i\,\frac{\varepsilon_\alpha^R}{\hbar\omega}\,\phi\right), \tag{7}$$

with *quasienergies* ε_α^R and functions $|u_\alpha^R(\phi)\rangle$ that inherit the 2π-periodicity of $K^R(\phi)$,

$$|u_\alpha^R(\phi)\rangle = |u_\alpha^R(\phi + 2\pi)\rangle. \tag{8}$$

We briefly recollect some properties of the Floquet states that will be indispensable in the following [8]. Since each such state solves the time-dependent Schrödinger equation with the fixed-parameter Hamiltonian $K^R(\phi)$, *i.e.*,

$$i\frac{d}{d\phi}|\psi_\alpha^R(\phi)\rangle = K^R(\phi)|\psi_\alpha^R(\phi)\rangle, \tag{9}$$

one immediately gets

$$\left(K^R(\phi) - i\frac{d}{d\phi}\right)|u_\alpha^R(\phi)\rangle = \frac{\varepsilon_\alpha^R}{\hbar\omega}\,|u_\alpha^R(\phi)\rangle. \tag{10}$$

These are eigenvalue equations for quasienergies and Floquet functions at the respective parameters R, posed in an *extended Hilbert space* consisting of 2π-periodic functions [9]. This Hilbert space is naturally equipped with the scalar product

$$\langle\langle u_\alpha^R|v_\beta^R\rangle\rangle = \frac{1}{2\pi}\int_0^{2\pi} d\phi\ \langle u_\alpha^R(\phi)|v_\beta^R(\phi)\rangle, \tag{11}$$

where $\langle\,\cdot\,|\,\cdot\,\rangle$ denotes the usual scalar product in the space spanned by the eigenstates of H_0.

An important point to be noted here is the Brillouin-zone structure of the solutions to these eigenvalue problems (10): if $|u_n^R(\phi)\rangle$ is an eigenfunction with quasienergy ε_n^R, then also $|u_n^R(\phi)e^{im\phi}\rangle$ is an eigenfunction, with quasienergy $\varepsilon_n^R + m\hbar\omega$. The requirement that the eigenfunctions are 2π-periodic restricts m to (positive or negative) integer numbers. However, all eigenfunctions that can be obtained by multiplying a given $|u_n^R(\phi)\rangle$ by a factor $e^{im\phi}$ belong to the *same* Floquet state, since obviously

$$|u_n^R(\phi)e^{im\phi}\rangle \exp\left(-i\,\frac{\varepsilon_n^R + m\hbar\omega}{\hbar\omega}\,\phi\right) = |u_n^R(\phi)\rangle \exp\left(-i\,\frac{\varepsilon_n^R}{\hbar\omega}\,\phi\right). \tag{12}$$

Hence, the index α that labels the solutions to the eigenvalue problem (10) has to be understood as a double-index:

$$\alpha = (n,m),\quad n = 1,\ldots,N;\quad m = 0,\pm1,\pm2,\ldots, \tag{13}$$

with n counting the N Floquet states to the 2π-periodic N-level Hamiltonian (5), and m accounting for the mod $\hbar\omega$-multiplicity of the quasienergies that is introduced by factorizing a Floquet state (7) into a 2π-periodic eigenfunction to the problem (10) and an exponential. In other words, there is a whole *class* of eigensolutions to (10), labeled by n, that corresponds to a single physical Floquet state; the individual members of this class are distinguished by the second quantum number m. Correspondingly, the quasienergy of a Floquet state is determined only up to an integer multiple of $\hbar\omega$.

This observation gives rise to two different notions of completeness, both of which will become important in the following. On the one hand, the N linearly independent Floquet states are complete, at each instant ϕ, in the N-dimensional Hilbert space spanned by the eigenstates of H_0,

$$\sum_{n=1}^{N} |u_n^R(\phi)\rangle\langle u_n^R(\phi)| = \mathbf{1}. \tag{14}$$

Hence, each solution $|\psi(\phi)\rangle$ to the fixed-parameter Schrödinger equation (9) can be expanded, with ϕ-independent coefficients a_n, according to

$$|\psi(\phi)\rangle = \sum_{n=1}^{N} a_n \, |u_n^R(\phi)\rangle \exp\left(-i \, \frac{\varepsilon_n^R}{\hbar\omega} \, \phi\right), \tag{15}$$

where we have used the index n as a shorthand for $(n, 0)$, indicating that *only one* representative from each class of eigensolutions to (10) is needed here. On the other hand, *all* solutions to (10) are required for the completeness relation in the extended Hilbert space,

$$\sum_{n=1}^{N} \sum_{m=-\infty}^{+\infty} |u_n^R(\phi)\rangle\langle u_n^R(\phi')| \, e^{im(\phi-\phi')} = \mathbf{1} \cdot 2\pi\delta_{2\pi}(\phi - \phi'), \tag{16}$$

where $\delta_{2\pi}(\phi)$ denotes the 2π-periodic δ-function.

2.2 The adiabatic principle

The fact that the expansion coefficients a_n in equation (15) are ϕ- (*i.e.*, time-) independent underlies the usefulness of the Floquet states for the analysis of the dynamics induced by a strictly time-periodic Hamiltonian. When expanding the same wave function (15) with respect to the eigenstates of H_0, the expansion coefficients vary with time in a complicated manner. In contrast, once the Floquet states have been computed, and the initial wave function has been expanded in the Floquet basis, the wave function (15) is known for all times.

However, we are not primarily interested in the dynamics governed by a 2π-periodic Hamiltonian $K^R(\phi)$, but rather in the solutions to the Schrödinger equation (3) with the "slowly" varying Hamiltonian $H(t) = \hbar\omega(t)\, K^{R(\phi(t))}(\phi(t))$, where the curve $R(\phi)$ in parameter space specifies the laser pulse. To connect this pulse problem to the set of all Floquet eigenvalue problems that emerge by "freezing" $R(\phi)$ at some instantaneous value, we introduce a further phase variable p, formally independent of ϕ, and construct an "extended" Hamiltonian $K^{R(p)}(\phi)$:

$$K^{R(p)}(\phi) = (\hbar\omega(p))^{-1}(H_0 + \widehat{\mu}F(p)\sin(\phi)), \tag{17}$$

which has the important properties that it is 2π-periodic in ϕ for each fixed p, and that changing p accounts for the parameter variation during the pulse.

Next, we introduce a wave function $|\Psi(\phi, p)\rangle$ which equals the physical wave function $|\psi(\phi)\rangle$ on the diagonal $p = \phi$ [10,11],

$$|\Psi(\phi, \phi)\rangle = |\psi(\phi)\rangle. \tag{18}$$

The Schrödinger equation with moving parameters,

$$i\frac{d}{d\phi}|\psi(\phi)\rangle = K^{R(\phi)}(\phi)|\psi(\phi)\rangle\,, \tag{19}$$

then translates into

$$\left[i\frac{\partial}{\partial\phi}|\Psi(\phi,p)\rangle + i\frac{\partial}{\partial p}|\Psi(\phi,p)\rangle\right]_{p=\phi} = K^{R(p)}(\phi)|\Psi(\phi,p)\rangle\Big|_{p=\phi}. \tag{20}$$

Requiring the validity of this equation even for $p \neq \phi$, one obtains the evolution equation [5,6]

$$i\frac{\partial}{\partial p}|\Psi(\phi,p)\rangle = \mathcal{K}(\phi,p)|\Psi(\phi,p)\rangle, \tag{21}$$

where we have introduced the operator

$$\mathcal{K}(\phi,p) \equiv K^{R(p)}(\phi) - i\frac{\partial}{\partial\phi}\,. \tag{22}$$

This evolution equation distinguishes the short time scale $T = 2\pi/\omega$, associated with ϕ, from the comparatively long time scale that characterizes the change of the pulse parameters R, associated with p. We remark that also the so-called $(t-t')$ method, which has been designed for the numerical solution of the Schrödinger equation [12], makes similar use of two time variables.

We are now in a position to apply the adiabatic theorem of quantum mechanics [13–16] to this equation (21). To this end, we first have to find the eigenstates and eigenvalues of the operator $\mathcal{K}(\phi, p)$ for each fixed parameter combination R that lies on the curve $R(p)$. This means nothing but solving all the eigenvalue problems (10), *i.e.*, determining the instantaneous Floquet states. We require that these states be properly normalized with respect to the scalar product (11). This requirement still leaves the phases of the instantaneous Floquet states unspecified at each R. We fix these phases, up to an overall phase for each state, by demanding

$$\langle\langle u_\alpha^{R(p)}|\nabla_R \, u_\alpha^{R(p)}\rangle\rangle\dot{R}(p) = 0. \tag{23}$$

This is where the change from the original time variable t to the phase ϕ becomes crucial. When working with t, one encounters extended Hilbert spaces spanned by the sets $\{|n\rangle e^{im\omega t}\}$, which means that a frequency chirp affects the basis vectors. In contrast, when working with ϕ, there is just a single extended Hilbert space spanned by $\{|n\rangle e^{im\phi}\}$, and the requirement (23) – paralleling directly the fixing of the instantaneous eigenstates' phases in the familiar formulations of the adiabatic theorem [13–16] – corresponds to parallel transport [17] in this extended space. Moreover,

we stipulate that different Floquet eigenfunctions belonging to the same Floquet state (*i.e.*, eigenfunctions labeled by the same index n, but different m), differ merely by the phase factor $e^{im\phi}$, thus excluding an additional constant phase. It is then clear that all members of a class of Floquet functions respect equation (23), if one does.

For convenience, we now set $\phi(t_i) = 0$. The adiabatic theorem [13–16], applied to the evolution equation (21), then states that given an initial function

$$|\Psi(\phi, p = 0)\rangle = \sum_\alpha c_\alpha |u_\alpha^{R(0)}(\phi)\rangle, \tag{24}$$

this function will evolve with p according to

$$|\Psi(\phi, p)\rangle = \sum_\alpha c_\alpha |u_\alpha^{R(p)}(\phi)\rangle \exp\left(-i \int_0^p dp' \, \frac{\varepsilon_\alpha^{R(p')}}{\hbar\omega(p')}\right) \tag{25}$$

in the adiabatic limit of "infinitely slow" parameter variation, so that the expansion coefficients c_α remain constant, provided the instantaneous quasienergies ε_α^R remain nondegenerate along the path $R(p)$. Note that this application of the adiabatic theorem involves *all* solutions to the eigenvalue equation (10), as expressed by the appearance of the double index α.

In order to exploit this adiabatic principle for the solution of the original Schrödinger equation (3) that one is actually interested in, we first have to "lift" the initial state

$$|\psi(\phi = 0)\rangle = \sum_{n=1}^{N} a_n |u_n^{R(0)}(0)\rangle \tag{26}$$

to the extended Hilbert space. This procedure is *not unique*: all functions

$$\begin{aligned} |\Psi(\phi, p = 0)\rangle &= \sum_\alpha c_\alpha |u_\alpha^{R(0)}(\phi)\rangle \\ &= \sum_{n=1}^{N} \sum_{m=-\infty}^{+\infty} c_{(n,m)} |u_{(n,0)}^{R(0)}(\phi) e^{im\phi}\rangle \end{aligned} \tag{27}$$

correspond to $|\psi(\phi = 0)\rangle$, if only

$$\sum_{m=-\infty}^{+\infty} c_{(n,m)} = a_n \tag{28}$$

for $n = 1, \ldots, N$. Therefore, it has to be guaranteed that the final wave function $|\psi(\phi_f))\rangle$ that results from lifting the initial state, adiabatically transporting in the extended Hilbert space, and back-projecting by setting $p = \phi_f$, does not depend on the particular choice of the coefficients $c_{(n,m)}$, provided they comply with (28). But this can easily be seen: resolving the double index α, the transported wave function (25) becomes

$$\begin{aligned} |\Psi(\phi, p)\rangle = \sum_{n=1}^{N} \sum_{m=-\infty}^{+\infty} c_{(n,m)} |u_{(n,0)}^{R(p)}(\phi) e^{im\phi}\rangle \\ \times \exp\left(-i \int_0^p dp' \, \frac{\varepsilon_{(n,0)}^{R(p')}}{\hbar\omega(p')} - imp\right). \end{aligned} \tag{29}$$

After projection, this gives the *unique* adiabatic approximation

$$|\psi(\phi_f)\rangle = \sum_{n=1}^{N} a_n |u_n^{R(\phi_f)}(\phi_f)\rangle \exp\left(-i \int_0^{\phi_f} d\phi \, \frac{\varepsilon_n^{R(\phi)}}{\hbar\omega(\phi)}\right) \tag{30}$$

to the Schrödinger wave function, using equation (28) and again writing n for $(n, 0)$. The simplicity of this consistency check rests once more on the use of the variable ϕ instead of t.

3 Adiabatic perturbation theory for Floquet states

The tool for understanding the deviations from strictly adiabatic motion that will necessarily emerge when the pulse parameters do *not* vary "infinitely slowly" is time-dependent perturbation theory in the adiabatic basis. We split the treatment into three parts, and consider deviations that occur during the pulse, when there are no near-degeneracies of instantaneous quasienergies, deviations that stem from the way the pulse is switched on and off and remain visible at the end of the pulse, and Landau-Zener transitions of Floquet states at avoided crossings of quasienergies.

3.1 Transition probabilities during the pulse

We assume that at the beginning of the pulse (when the pulse's amplitude still vanishes, so that the Floquet states coincide with the eigenstates of the unperturbed Hamiltonian H_0) only a single eigenstate of H_0 is populated,

$$|\psi(\phi = 0)\rangle = |u_1^{R(0)}(0)\rangle, \tag{31}$$

lift this wave function to the extended Hilbert space,

$$|\Psi(\phi, p = 0)\rangle = |u_{(1,0)}^{R(0)}(\phi)\rangle, \tag{32}$$

and consider the *exact* wave function

$$|\Psi(\phi, p)\rangle = \sum_\alpha c_\alpha(p) |u_\alpha^{R(p)}(\phi)\rangle \exp\left(-i \int_0^p dp' \, \frac{\varepsilon_\alpha^{R(p')}}{\hbar\omega(p')}\right) \tag{33}$$

that evolves from this initial state under the influence of the pulse. Note that we have done the lifting, without loss

of generality, by going from $a_n(0) = \delta_{n,1}$ to $c_{(n,m)}(0) = \delta_{n,1}\delta_{m,0}$ (*i.e.*, we have not spread the initial amplitude over more than one mode belonging to the Floquet state $n = 1$), but that, nonetheless, *all* indices α are needed in the expansion (33), since we now rely on the completeness (16) in the extended Hilbert space.

The expansion coefficients then obey the infinite system of equations

$$\partial_p c_\alpha(p) = -\sum_\beta c_\beta(p)\langle\langle u_\alpha^{R(p)}|\partial_p|u_\beta^{R(p)}\rangle\rangle \times \exp\left(-i\int_0^p dp'\,\frac{\varepsilon_\beta^{R(p')} - \varepsilon_\alpha^{R(p')}}{\hbar\omega(p')}\right), \qquad (34)$$

where we have used the symbol ∂_p to indicate the derivative with respect to the evolution variable p, and the double brackets indicate the scalar product (11). First-order perturbation theory amounts to replacing $c_\beta(p)$ by the initial values $c_{(n,m)}(0) = \delta_{n,1}\delta_{m,0}$, hence

$$c_\alpha(p) = -\int_0^p dp'\,\langle\langle u_\alpha^{R(p')}|\partial_{p'}|u_{(1,0)}^{R(p')}\rangle\rangle \times \exp\left(-i\int_0^{p'} dp''\,\frac{\varepsilon_{(1,0)}^{R(p'')} - \varepsilon_\alpha^{R(p'')}}{\hbar\omega(p'')}\right) \qquad (35)$$

for $\alpha \neq (1,0)$. This integral, with its fast-oscillating integrand, is difficult to evaluate as it stands, but successive partial integrations yield a systematic expansion in powers of $\hbar$ [18–20]. The first such step results in

$$\begin{aligned} c_\alpha(p) = {} & -i\hbar\omega(p')\frac{\langle\langle u_\alpha^{R(p')}|\partial_{p'}|u_{(1,0)}^{R(p')}\rangle\rangle}{\varepsilon_{(1,0)}^{R(p')} - \varepsilon_\alpha^{R(p')}} \times \exp\left(-i\int_0^{p'} dp''\,\frac{\varepsilon_{(1,0)}^{R(p'')} - \varepsilon_\alpha^{R(p'')}}{\hbar\omega(p'')}\right)\Bigg|_0^p \\ & + \int_0^p dp'\,\left(\partial_{p'}\left[i\hbar\omega(p')\frac{\langle\langle u_\alpha^{R(p')}|\partial_{p'}|u_{(1,0)}^{R(p')}\rangle\rangle}{\varepsilon_{(1,0)}^{R(p')} - \varepsilon_\alpha^{R(p')}}\right]\right) \\ & \times \exp\left(-i\int_0^{p'} dp''\,\frac{\varepsilon_{(1,0)}^{R(p'')} - \varepsilon_\alpha^{R(p'')}}{\hbar\omega(p'')}\right). \end{aligned} \qquad (36)$$

Upon further partial integration, the remaining integral then produces terms proportional to $\hbar^2$ and another integral, and so on. However, since the expression (36) has been obtained within first-order perturbation theory from equation (34), only the $O(\hbar)$-term is consistent here; computing higher-order terms requires higher-order perturbation theory right from the outset.

Within the first-order approximation, we therefore keep only the $O(\hbar)$-term in equation (36). For calculating the amplitudes $a_n(\phi)$ in the expansion

$$|\psi(\phi)\rangle = \sum_{n=1}^N a_n(\phi)|u_n^{R(\phi)}(\phi)\rangle\exp\left(-i\int_0^\phi d\phi'\,\frac{\varepsilon_n^{R(\phi')}}{\hbar\omega(\phi')}\right), \qquad (37)$$

and hence the occupation probabilities $|a_n(\phi)|^2$ of the instantaneous Floquet states during the pulse, subject to the initial condition $a_n(0) = \delta_{n,1}$, we have to return to the physical Hilbert space by setting $p = \phi$, and to sum over all the modes that make up the nth Floquet state. Assuming that there is no contribution from $p = 0$ (which is the case, *e.g.*, if the envelope function $F(p)$ is continuously differentiable at $p = 0$, see following subsection), we find

$$\begin{aligned} |a_n(\phi)|^2 &= \hbar^2\omega^2(\phi)\left|\sum_{m=-\infty}^{+\infty}\frac{\langle\langle u_{(n,m)}^{R(p)}|\partial_p|u_{(1,0)}^{R(p)}\rangle\rangle_{p=\phi}}{\varepsilon_{(1,0)}^{R(\phi)} - \varepsilon_{(n,m)}^{R(\phi)}} \times \exp\left(-i\int_0^\phi d\phi'\,\frac{\varepsilon_{(1,0)}^{R(\phi')} - \varepsilon_{(n,m)}^{R(\phi')}}{\hbar\omega(\phi')}\right)\right|^2 \\ &= \hbar^2\omega^2(\phi)\left|\sum_{m=-\infty}^{+\infty}\frac{\langle\langle u_{(n,m)}^{R(p)}|\partial_p|u_{(1,0)}^{R(p)}\rangle\rangle_{p=\phi}}{\varepsilon_{(1,0)}^{R(\phi)} - \varepsilon_{(n,m)}^{R(\phi)}}\,e^{im\phi}\right|^2 \end{aligned} \qquad (38)$$

for $n \neq 1$. Hence, even when tracked in the adiabatic basis, the instantaneous occupation probabilities exhibit oscillations that result from the periodic driving. At this point the Brillouin-zone structure of the eigenvalue problem (10), which remained invisible as long as the parameters were kept fixed, shows up: it is the interference of different modes belonging to the same Floquet state that is responsible for the oscillations of the transition probabilities.

To see what this means in practice, we consider a pulsed two-level system with separation ΔE between the unperturbed energy levels:

$$H(t) = \frac{\Delta E}{2}\sigma_z + \mu F(t)\sin(\phi(t))\sigma_x\,, \qquad (39)$$

where σ_x and σ_z denote the usual Pauli matrices; $\mu\sigma_x = \widehat{\mu}$ is the dipole operator. We set $\phi(t) = \omega t$, *i.e.*, we keep the frequency ω fixed, and study the response to pulses of the form

$$F(t) = F_{max}\sin^2(\pi t/T_{pulse}) \qquad (40)$$

for $0 = t_i \leq t \leq T_{pulse} = t_f$. Figure 1 shows the quasienergies for $\Delta E/(\hbar\omega) = 2.2$ as functions of the instantaneous field strength F. Since the driving frequency ω is smaller than $\Delta E/\hbar$, the ac Stark shift pushes the two levels with increasing field strength further apart, until one meets a three-photon resonance, which manifests itself as the avoided quasienergy crossing at $\mu F/(\hbar\omega) \approx 1.33$. We stay clear of this resonance by choosing $\mu F_{max}/(\hbar\omega) = 0.8$. The full line in the upper panel of Figure 2 then shows the transition probability $|a_2(t)|^2$ obtained by numerically solving the Schrödinger equation for a pulse with a length of merely 20 cycles, $T_{pulse} = 20\,(2\pi/\omega) \equiv 20\,T$; the initial condition was $a_n(0) = \delta_{n,1}$. As expected from equation (38), the probability oscillates with period $T/2$. The lower panel depicts the absolute squares of the dominant

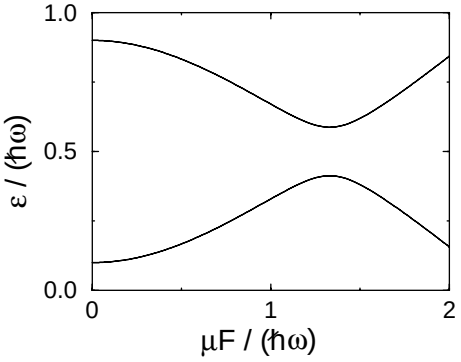

Fig. 1. Quasienergies for the two-level system (39) with fixed frequency ω, and $\Delta E/(\hbar\omega) = 2.2$.

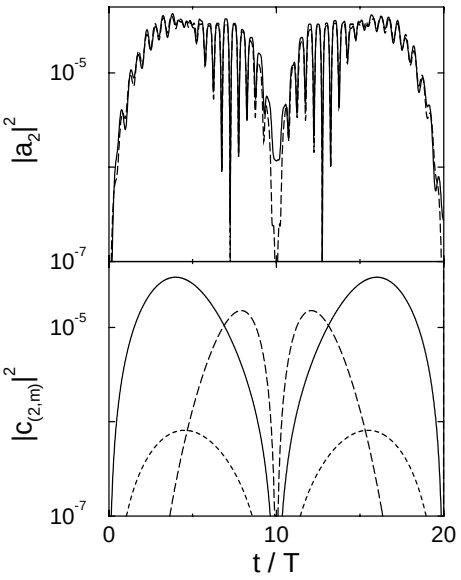

Fig. 2. Upper panel: numerically computed exact transition probability $|a_2(t)|^2$ (full line) for a two-level system (39) subjected to a pulse (40) with constant frequency ω; parameters are $\Delta E/(\hbar\omega) = 2.2$, $\mu F_{max}/(\hbar\omega) = 0.8$, and $T_{pulse} = 20\,(2\pi/\omega) \equiv 20\,T$. The dashed line results from first-order perturbation theory; see equation (38). Lower panel: dominant modes $c_{(2,m)}(t)$ for the expansion (33) in the extended Hilbert space.

expansion coefficients $c_{(2,m)}(t)$ in the extended Hilbert space as obtained from the $O(\hbar)$-term in equation (36); the dashed line in the upper panel – almost indistinguishable from the full line – shows what results from their coherent summation according to equation (38). Obviously, first-order adiabatic perturbation theory captures the exact transition probabilities very well, even though the pulse is by no means long, that is, the envelope $F(t)$ is not really slowly varying: it reaches its maximum amplitude already after 10 cycles. It is also interesting to see that the only significant deviation of the perturbative result from the exact one occurs in the middle of the pulse. This is due to the fact that the first derivative of the envelope function vanishes here, so that the result of the first-order calculation vanishes too (see Eq. (42) below); correcting this shortcoming requires a higher-order calculation.

3.2 Non-smoothness at the pulse ends

We now focus on deviations from adiabaticity that are caused by some non-smoothness at the beginning or end of the pulse. An example for this is provided already by the envelope (40): when continued by $F(t) \equiv 0$ for $t < 0$ and $t > T_{pulse}$, it is once, but not twice, continuously differentiable at the pulse ends. Consequences of such a roughness have been studied by Garrido and Sancho [21] and Sancho [22] in the context of merely parametrically time-dependent quantum systems, without periodic forcing.

Let us assume that the first $j-1$ derivatives of the envelope function $F(p)$ vanish at the pulse ends, and that $F^{(j)}(0+) \neq 0$ and/or $F^{(j)}(p_f-) \neq 0$. Switching again to the variable ϕ, with $\phi(t_i) = 0$ and $\phi(t_f) = \phi_f$, and starting from the first-order approximation (35), the leading contribution to the transition amplitude is obtained after integrating j times by parts:

$$c_\alpha(p_f) = (-1)^j \left[\left(\frac{i\hbar\omega(p)}{\varepsilon^{R(p)}_{(1,0)} - \varepsilon^{R(p)}_\alpha} \partial_p \right)^{j-1} \frac{i\hbar\omega(p) \langle\langle u^{R(p)}_\alpha | \partial_p | u^{R(p)}_{(1,0)} \rangle\rangle}{\varepsilon^{R(p)}_{(1,0)} - \varepsilon^{R(p)}_\alpha} \right] \times \exp\left(-i \int_0^p dp' \, \frac{\varepsilon^{R(p')}_{(1,0)} - \varepsilon^{R(p')}_\alpha}{\hbar\omega(p')} \right) \Bigg|_0^{p_f} \quad (41)$$

for $\alpha \neq (1,0)$. Next, we use the identity

$$\langle\langle u^{R(p)}_\alpha | \partial_p | u^{R(p)}_\beta \rangle\rangle = \hbar\omega(p) \frac{\langle\langle u^{R(p)}_\alpha | \partial_p \mathcal{K} | u^{R(p)}_\beta \rangle\rangle}{\varepsilon^{R(p)}_\beta - \varepsilon^{R(p)}_\alpha} \quad (\alpha \neq \beta). \quad (42)$$

Since $\langle\langle u^{R(p)}_\alpha | \partial^\ell_p \mathcal{K} | u^{R(p)}_\beta \rangle\rangle = 0$ for $\ell < j$ and $p = 0, p_f$ by assumption, a non-vanishing contribution to $c_\alpha(p_f)$ can result only if ∂_p acts j times directly on $\mathcal{K}$. Hence, we find

$$c_\alpha(p_f) = (-i)^j \left(\frac{\hbar\omega(p)}{\varepsilon^{R(p)}_{(1,0)} - \varepsilon^{R(p)}_\alpha} \right)^{j+1} \langle\langle u^{R(p)}_\alpha | \partial^j_p \mathcal{K} | u^{R(p)}_{(1,0)} \rangle\rangle \times \exp\left(-i \int_0^p dp' \, \frac{\varepsilon^{R(p')}_{(1,0)} - \varepsilon^{R(p')}_\alpha}{\hbar\omega(p')} \right) \Bigg|_0^{p_f} . \quad (43)$$

At the pulse ends $p = 0$ and $p = p_f$ we have $|u^{R(0)}_\alpha(\phi)\rangle = |n\, e^{im\phi}\rangle$, $|u^{R(p_f)}_\alpha(\phi)\rangle = |n\, e^{im\phi}\rangle e^{i\gamma_n}$, and $\varepsilon^{R(p)}_\alpha = E_n + m\hbar\omega(p)$, where $|n\rangle$ and E_n denote the eigenstates and eigenvalues of H_0, respectively. The real numbers γ_n are

$$|a_n(\phi_f)|^2 = \frac{|\langle n|\widehat{\mu}|1\rangle|^2}{4} \left| \frac{(\hbar\omega(\phi_f))^j e^{i(\gamma_1-\gamma_n+\phi_f)}}{(E_n+\hbar\omega(\phi_f)-E_1)^{j+1}}\, F^{(j)}(\phi_f-) \exp\left(-i\int_0^{\phi_f} d\phi \frac{\varepsilon^{R(\phi)}_{(1,0)}-\varepsilon^{R(\phi)}_{(n,0)}}{\hbar\omega(\phi)}\right) - \frac{(\hbar\omega(0))^j}{(E_n+\hbar\omega(0)-E_1)^{j+1}}\, F^{(j)}(0+) \right.$$
$$\left. - \frac{(\hbar\omega(\phi_f))^j\, e^{i(\gamma_1-\gamma_n-\phi_f)}}{(E_n-\hbar\omega(\phi_f)-E_1)^{j+1}}\, F^{(j)}(\phi_f-) \exp\left(-i\int_0^{\phi_f} d\phi\, \frac{\varepsilon^{R(\phi)}_{(1,0)}-\varepsilon^{R(\phi)}_{(n,0)}}{\hbar\omega(\phi)}\right) + \frac{(\hbar\omega(0))^j}{(E_n-\hbar\omega(0)-E_1)^{j+1}}\, F^{(j)}(0+) \right|^2 . \quad (45)$$

geometrical Berry phases [23], resulting from the parallel transport (23). Hence,

$$\langle\langle u^{R(0)}_\alpha | \partial_p^j \mathcal{K} | u^{R(0)}_{(1,0)}\rangle\rangle = \frac{1}{\hbar\omega(0)} \langle n|\widehat{\mu}|1\rangle\, F^{(j)}(0)\, \frac{1}{2i}\, (\delta_{m,1}-\delta_{m,-1})\,; \quad (44)$$

for $p = p_f$ one also gets a Berry phase factor $e^{i(\gamma_1-\gamma_n)}$. Since the sinusoidal driving described by the quasienergy operator $\mathcal{K}$ connects only neighboring modes, *i.e.*, modes differing in m by ± 1, the final transition probabilities $|a_n(\phi_f)|^2$ for $n \neq 1$ become

see equation (45) above.

This formula has a transparent structure: each of the two modes contributing to the final transition probability picks up contributions originating from the non-smoothness at both the beginning and at the end of the pulse; the latter are accompanied by the dynamical and geometrical phases that result from evolving the wave function over the whole pulse. The dynamical phases are determined by the quasienergies, reflecting adiabatic transport of Floquet states during the pulse; the geometrical phases express the possible anholonomy of this transport [17,23].

Figure 3 shows a comparison of the perturbative result (45) with exact numerical data, again for the two-level system (39) with the envelope function (40) and constant frequency ω, so that $j = 2$. In this case the geometrical phases vanish. We now have chosen $\mu F_{max}/(\hbar\omega) = 0.1$ and $\Delta E/(\hbar\omega) = 0.2$. The analytical approximation to $|a_2(T_{pulse})|^2$ starts to agree very well with the exact data already for pulses which are merely two cycles long, which again underlines the usefulness of adiabatic Floquet state perturbation theory even for really short pulses.

Evidently, the total non-adiabatic loss of probability from the initially populated state $n = 1$ that is caused by the non-smoothness at the onset of the pulse is given by

$$\sum_{n=2}^{N} |a_n(0+)|^2 = \frac{1}{4}(\hbar\omega(0))^{2j} \sum_{n=2}^{N} \left| \frac{F^{(j)}(0+)\,\langle n|\widehat{\mu}|1\rangle}{(E_n+\hbar\omega(0)-E_1)^{j+1}} - \frac{F^{(j)}(0+)\,\langle n|\widehat{\mu}|1\rangle}{(E_n-\hbar\omega(0)-E_1)^{j+1}} \right|^2 . \quad (46)$$

Thus, if the turn-on of the pulse is somewhat rough, a certain amount of probability is lost for the intended adiabatic transfer right from the beginning. We will return to this expression (46) in the following section, where we analyze pulse dynamics with the help of superadiabatic techniques.

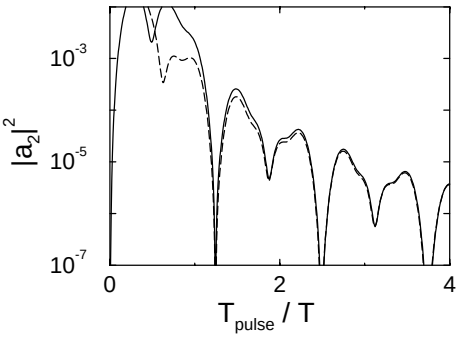

Fig. 3. Comparison of the perturbative prediction (45) for the final transition probability $|a_2(T_{pulse})|^2$ in a pulsed two-level system (39) (dashed) with exact numerical data (full line), for pulses no longer than merely 4 cycles $T = 2\pi/\omega$. The frequency ω is kept constant; the pulse shape is given by equation (40). Parameters are $\Delta E/(\hbar\omega) = 0.2$ and $\mu F_{max}/(\hbar\omega) = 0.1$.

3.3 Landau-Zener transitions among Floquet states

Near-degeneracies of instantaneous quasienergies during the pulse are of particular interest, since they lead to comparatively simple and robust strategies for controlling the outcome of the pulse by suitably adjusting its parameters.

We consider an avoided crossing between the quasienergy $\varepsilon^R_{(1,0)}$ originating from the energy of the initially occupied state, and some other quasienergy ε^R_α. More specifically, we assume that the variation of the instantaneous quasienergies as seen by the system in the course of time is of the Landau-Zener form [24,25],

$$\begin{aligned} \varepsilon^{R(t)}_{(1,0)} &= \tfrac{1}{2}\sqrt{(\delta\varepsilon)^2+\gamma^2(t-t_0)^2} \equiv \varepsilon_+(t) \\ \varepsilon^{R(t)}_{\alpha} &= -\varepsilon^{R(t)}_{(1,0)} \qquad\qquad\quad \equiv \varepsilon_-(t), \end{aligned} \quad (47)$$

so that an avoided quasienergy crossing of width $\delta\varepsilon$ is encountered at $t = t_0$; we are free to set $t_0 = 0$. Within the first-order approximation (35), the amplitude of the anticrossing state after the passage of the avoided crossing is then given by

$$c_\alpha(+\infty) = -\int_{-\infty}^{+\infty} dt\, \langle\langle u^{R(t)}_\alpha | \partial_t | u^{R(t)}_{(1,0)}\rangle\rangle \times \exp\left(-\frac{i}{\hbar}\int_0^t dt'\, (\varepsilon_+(t')-\varepsilon_-(t'))\right), \quad (48)$$

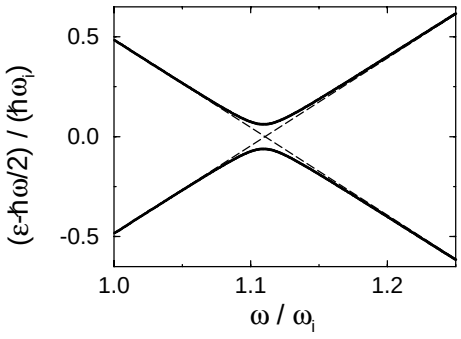

Fig. 4. Instantaneous quasienergies (full lines) for the driven two-level system (39) with fixed amplitude $\mu F/(\hbar\omega_i) = 6.089$. The reference frequency ω_i is given by $\Delta E/(\hbar\omega_i) = 5.556$, so that the avoided crossing corresponds to a five-photon resonance. The width of the avoided crossing is $\delta\varepsilon/(\hbar\omega_i) = 0.1236$; the total diabatic quasienergy variation for $\omega_f/\omega_i = 1.25$ is $\Delta\varepsilon/(\hbar\omega_i) = 1.1004$. The asymptotes confirm that the five-photon transition induced by a linear frequency chirp is of the Landau-Zener type.

apart from an irrelevant phase factor. Now we can adopt standard arguments [18,26]: introducing the variable

$$w(t) = \frac{1}{\hbar}\int_0^t dt' \left(\varepsilon_+(t') - \varepsilon_-(t')\right) = \frac{t}{2\hbar}\sqrt{(\delta\varepsilon)^2 + (\gamma t)^2} + \frac{(\delta\varepsilon)^2}{2\hbar\gamma}\mathrm{arcsinh}\left(\frac{\gamma t}{\delta\varepsilon}\right), \quad (49)$$

the complex degeneracy point $t_c = -i\,\delta\varepsilon/\gamma$ of the quasienergies $\varepsilon_+(t)$ and $\varepsilon_-(t)$ corresponds to

$$w(t_c) \equiv w_c = -i\frac{\pi}{4}\frac{(\delta\varepsilon)^2}{\hbar\gamma}, \quad (50)$$

and the expression (48) can be brought into the universal form [18,26]

$$c_\alpha(+\infty) = \int_{-\infty}^{+\infty} dw\, \frac{i}{6(w - w_c)}\exp(-iw). \quad (51)$$

Closing the contour of integration by an infinitely large semi-circle in the lower half of the complex w-plane immediately gives

$$c_\alpha(+\infty) = \frac{\pi}{3}\exp(-iw_c). \quad (52)$$

The prefactor $\pi/3 \approx 1.047$ appearing in the present first-order analysis is changed to unity when the perturbation series is summed to all orders [18,26,27], so that the correct probability for a Landau-Zener transition among the anticrossing Floquet states becomes

$$P_{LZ} = \exp(-2|w_c|) = \exp\left(-\frac{\pi}{2}\frac{(\delta\varepsilon)^2}{\hbar\gamma}\right). \quad (53)$$

The remarkable point here is that we are treating Landau-Zener transitions in systems of the type (1) that vary both parametrically and periodically in time, that is, we have what is conventionally termed "multiphoton transitions" among Floquet states, but the use of the evolution equation (21), which underlies the expression (48), has allowed us to reduce this problem entirely to the usual analysis for Landau-Zener transitions among energy eigenstates. To demonstrate the accuracy of our arguments, we resort once more to the forced two-level system (39), keep the field strength fixed at $\mu F/(\hbar\omega_i) = 6.089$, and consider a linear frequency chirp

$$\omega(t) = \omega_i + \frac{t - t_i}{t_f - t_i}(\omega_f - \omega_i) \quad (54)$$

between times t_i and t_f, with $\Delta E/(\hbar\omega_i) = 5.556$ and $\Delta E/(\hbar\omega_f) = 4.444$. Thus, we are chirping over a five-photon resonance. In Figure 4 we depict the corresponding instantaneous quasienergies, shifted by $-\hbar\omega/2$ for graphical convenience.

Choosing the initial frequency ω_i as the reference frequency, and assuming that $(t_f - t_i) = r\,(2\pi/\omega_i)$, the Landau-Zener formula (53) can be written in the form

$$\frac{\ln P_{LZ}}{r} = -\frac{\pi^2}{2}\frac{(\delta\varepsilon/\hbar\omega_i)^2}{\Delta\varepsilon/\hbar\omega_i}, \quad (55)$$

where $\Delta\varepsilon$ is the *diabatic* quasienergy variation between times t_i and t_f, so that $\gamma/2 = \Delta\varepsilon/(t_f - t_i)$ in equation (53). From the data underlying Figure 4 one determines $\delta\varepsilon/(\hbar\omega_i) = 0.1236$ and $\Delta\varepsilon/(\hbar\omega_i) = 1.1004$; hence one expects $\ln P_{LZ}/r = -0.0685$. On the other hand, we have solved the time-dependent Schrödinger equation for the chirped two-level system by direct numerical integration in order to determine the Landau-Zener transition probabilities without approximation; the resulting data shown in Figure 5 give $\ln P_{LZ}/r = -0.0687$. The striking agreement with the theoretical expectation confirms that the reduction of the original Floquet-type transition problem to the usual Landau-Zener problem, which relies crucially on the evolution equation (21) in the extended Hilbert space, correctly captures the physics of chirp-induced multiphoton transitions.

4 Superadiabatic Floquet dynamics

To characterize the degree of adiabaticity when the laser pulses are short, we now replace the evolution variable p in equation (21) by q/η, and stipulate that q varies between 0 and 1 during the pulse, so that approaching the adiabatic limit means taking the dimensionless adiabaticity parameter η to zero. The evolution equation (21) then takes the form

$$i\eta\frac{\partial}{\partial q}|\Psi(\phi, q)\rangle = \mathcal{K}(\phi, q)|\Psi(\phi, q)\rangle, \quad (56)$$

with $|\Psi(\phi, q)\rangle$ and $\mathcal{K}(\phi, q)$ as shorthand notation for $|\Psi(\phi, q/\eta)\rangle$, $\mathcal{K}(\phi, q/\eta)$. As a consequence, the transition amplitudes considered in Sections 3.1 and 3.2 become

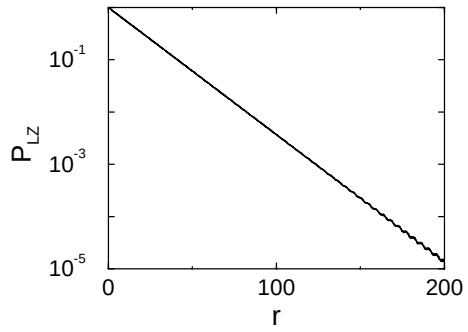

Fig. 5. Landau-Zener transition probabilities for the two-level system (39) with fixed amplitude $\mu F/(\hbar\omega_i) = 6.089$ and linear frequency chirp (54), corresponding to the avoided quasienergy crossing displayed in Figure 4. The data were obtained from numerical solutions of the time-dependent Schrödinger equation for chirps with duration $t_f - t_i = r\,(2\pi/\omega_i)$. The slope of the straight line is $\ln P_{LZ}/r = -0.0687$.

proportional to powers of η, whereas the Landau-Zener transition probability studied in Section 3.3 is of the order $O(\exp(-const/\eta))$. The guiding idea behind superadiabatic approaches to quantum dynamics [26–29] is to provide a series of successive unitary transformations to new frames of reference that are better adapted to the actual "fast" evolution than the adiabatic basis, such that in these new bases the contributions to the transition amplitude that are merely proportional to powers of η are removed. A very transparent formulation of this idea has been given by Berry [26] for parametrically time-dependent quantum systems. In this section we generalize his approach to laser-driven systems (1), and show that superadiabatic transformations furnish a diagnostic tool for optimizing laser pulses.

To this end, we try to represent the exact solution to equation (56) that emerges from the initial condition

$$|\Psi_\alpha(\phi,0)\rangle = |u_\alpha^{R(0)}(\phi)\rangle \tag{57}$$

by the power series

$$|\Psi_\alpha(\phi,q)\rangle = \exp\left(-\frac{i}{\eta}\int_0^q dq'\,\frac{\varepsilon_\alpha^{R(q')}}{\hbar\omega(q')}\right)\sum_{s=0}^{\infty}\eta^s\,|v_\alpha^{(s)}(\phi,q)\rangle, \tag{58}$$

where the functions $|v_\alpha^{(s)}(\phi,q)\rangle$ are linear combinations of the instantaneous Floquet functions:

$$|v_\alpha^{(s)}(\phi,q)\rangle = \sum_\beta a_{\alpha\beta}^{(s)}(q)\,|u_\beta^{R(q)}(\phi)\rangle\,, \tag{59}$$

with initial conditions

$$a_{\alpha\beta}^{(0)}(q) = \delta_{\alpha,\beta}, \tag{60}$$

so that $|v_\alpha^{(0)}(\phi,q)\rangle = |u_\alpha^{R(q)}(\phi)\rangle$, and

$$a_{\alpha\beta}^{(s)}(0) = 0 \qquad \text{for} \quad s > 0. \tag{61}$$

Inserting the ansatz (58) into the evolution equation (56) and comparing coefficients of equal powers of η, we obtain the recursive relations

$$a_{\alpha\beta}^{(s)}(q) = \frac{-i\hbar\omega(q)}{\varepsilon_\alpha^{R(q)} - \varepsilon_\beta^{R(q)}}\Big\{\partial_q a_{\alpha\beta}^{(s-1)}(q) + \sum_\gamma \langle\langle u_\beta^{R(q)}|\partial_q|u_\gamma^{R(q)}\rangle\rangle\, a_{\alpha\gamma}^{(s-1)}(q)\Big\} \quad (\alpha\neq\beta) \tag{62}$$

$$\partial_q a_{\alpha\alpha}^{(s)}(q) = -\sum_\beta \langle\langle u_\alpha^{R(q)}|\partial_q|u_\beta^{R(q)}\rangle\rangle a_{\alpha\beta}^{(s)}(q) \tag{63}$$

which are direct analogs of the corresponding relations for systems with merely a simple parametric time-dependence [27]. They allow us to determine the coefficients $a_{\alpha\beta}^{(s)}(q)$ required in equation (59), and hence the wave functions (58).

The desired sequence of superadiabatic bases $\{\,|\psi_n^{(S)}(\phi)\rangle\,\}$ $(S = 0, 1, 2\ldots)$ for monitoring the solutions to the original Schrödinger equation (3) is obtained by truncating the series (58) at $s = S$, and then returning to the physical Hilbert space by equating $q/\eta = \phi$:

$$|\psi_n^{(S)}(\phi)\rangle = \exp\left(-i\int_0^\phi d\phi'\,\frac{\varepsilon_n^{R(\phi')}}{\hbar\omega(\phi')}\right)\sum_{s=0}^{S}|v_n^{(s)}(\phi,\phi)\rangle. \tag{64}$$

Because of equation (60), the zeroth superadiabatic basis $(S = 0)$ coincides with the adiabatic basis itself.

Right from the outset, it is clear that the ansatz (58) will, in general, be divergent: it is merely a power series in η and thus cannot account for the Landau-Zener-type contributions to the transition amplitude, since these are "beyond all orders in η". However, the series is asymptotic [26]. Truncating at an optimal S_0, and expanding the Schrödinger wave function $|\psi(\phi)\rangle$ in that particular basis $\{\,|\psi_n^{(S_0)}(\phi)\rangle\,\}$, means disentangling the power-series contributions to the transition amplitude from the actually important Landau-Zener-type contributions, which then adopt a universal form [26]. In this way one isolates the essentials of the transition dynamics.

To explore how this works for laser-pulsed systems, we return to the two-level Hamiltonian (39) with pulse envelope (40) and fixed frequency ω. As in the situation studied in Figure 2, we set $\Delta E/(\hbar\omega) = 2.2$ and consider a pulse with a length of merely 20 cycles, but now the peak field strength is $\mu F_{max}/(\hbar\omega) = 1.5$, so that the avoided quasienergy crossing seen in Figure 1 is passed twice in the course of the pulse. Figure 6 shows the projection of the numerically computed solution $|\psi(t)\rangle$ to the Schrödinger equation (with bare state $|1\rangle$ as initial condition) onto the instantaneous adiabatic Floquet function $|u_2^{R(t)}(t)\rangle$ and onto the second-order superadiabatic basis vector $|\psi_2^{(2)}(t)\rangle$. A characteristic difference becomes visible at the beginning of the pulse: when measured in the adiabatic basis, the transition probability starts at

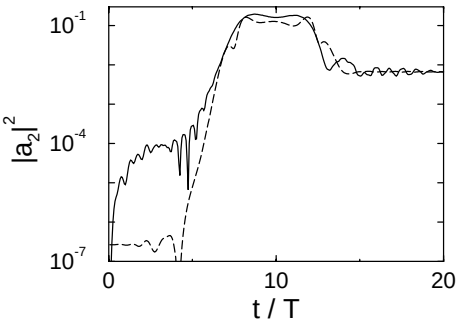

Fig. 6. Squared projection of the Schrödinger wave function $|\psi(t)\rangle$ evolving from the initial bare state $|1\rangle$ under the influence of a pulse (40) with constant frequency ω onto the zeroth-order superadiabatic basis vector $|u_2^{R(t)}(t)\rangle$ (full line), and onto the second-order superadiabatic basis vector $|\psi_2^{(2)}(t)\rangle$ (dashed). Parameters are $\Delta E/(\hbar\omega) = 2.2$ and $\mu F_{max}/(\hbar\omega) = 1.5$, so that the avoided crossing seen in Figure 1 is passed twice during the pulse; the pulse length is $T_{pulse} = 20\,T$.

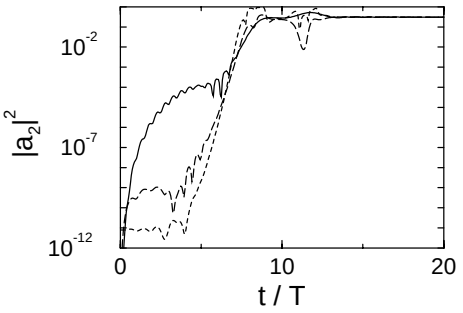

Fig. 7. As Figure 6, but for a pulse with the smoother envelope (65). The solution to the Schrödinger equation has been projected onto the adiabatic basis vector $|u_2^{R(t)}(t)\rangle$ (full line), onto the second-order superadiabatic basis vector $|\psi_2^{(2)}(t)\rangle$ (dashed), and onto the fourth-order superadiabatic basis vector $|\psi_2^{(4)}(t)\rangle$ (dotted).

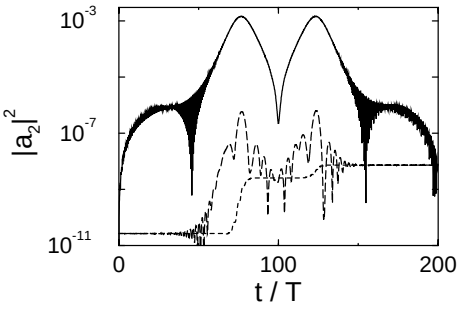

Fig. 8. Pulse dynamics for the driven two-level system (39) with parameters as in Figure 6, but for a pulse that is ten times longer, $T_{pulse} = 200\,T$. The transition probability is viewed in the adiabatic basis (full line; the black areas stem from oscillations of the type explained in Fig. 2), in the second-order superadiabatic basis (dashed), and in the tenth-order superadiabatic basis (dotted).

zero and reaches about 10^{-4} after a few cycles. In contrast, with respect to the second-order superadiabatic basis the probability remains initially constant at the value 2.640×10^{-7}. This is almost exactly equal to the value $|a_2(0+)|^2 = 2.641 \times 10^{-7}$ predicted by equation (46) as the non-adiabatic population loss due to the non-smoothness of the pulse envelope at the beginning: since the envelope is only once continuously differentiable, we have $j = 2$ in equation (46), so that the transition amplitude is affected to the order $O(\eta^2)$. The second-order superadiabatic basis is constructed such that this defect is taken out of the dynamics, so that the transition probability, viewed in this basis, initially stays constant at the value given by equation (46). The change of amplitude in the superadiabatic basis is caused mainly by the two passages through the avoided crossing at $t \approx 7.6\,T$ and $t \approx 12.4\,T$.

When changing the pulse envelope from (40) to

$$F(t) = F_{max} \sin^4(\pi t/T_{pulse}), \qquad 0 \le t \le T_{pulse}, \quad (65)$$

while keeping the parameters fixed, the initial non-adiabatic amplitude defect becomes proportional to η^4. It is then the fourth-order superadiabatic basis that best describes the dynamics during the initial stage of the pulse. This is illustrated in Figure 7, which compares the transition probability in the adiabatic basis to the probability viewed in the second-order and fourth-order superadiabatic bases. Note the change of the ordinate's scale as compared to the previous figure: the smoother the onset of the pulse, the less the initial non-adiabatic loss.

A striking example for the reduction to the essentials of the dynamics that can be achieved by superadiabatic transformations is displayed in Figure 8, where we consider a $\sin^2$-pulse that is 10 times longer than the one in Figure 6; the other parameters remain unchanged. In the adiabatic basis the final transition probability is reached after overshooting that final value by many orders of magnitude at the avoided crossings, and with the already familiar oscillations that stem from the interference of different Floquet modes, as in Figure 2. Viewed in higher-order superadiabatic bases, the dynamics become more and more simple. For $S = 2$ one still finds oscillations of the transition probability, now caused by the interference of a "perturbative" and a "non-perturbative" component [27], but the overshooting is already substantially diminished. For $S = 10$ the transition dynamics reduces to a mere sketch: starting with the value 2.6413×10^{-11} determined by the initial roughness of the pulse envelope (for comparison: equation (46) gives $|a_2(0+)|^2 = 2.6412 \times 10^{-11}$), the probability stays constant, apart from the two steps resulting from the passages through the avoided crossing. As can be deduced from Berry's theory [26], these steps, which mark the actual Landau-Zener induced probability loss, are universally approximated by error-functions.

As a further example for the use of superadiabatic transformations we study a chirp around the one-photon resonance of the two-level model (39). We choose the transition frequency $\omega_c = \Delta E/\hbar$ as reference frequency, take a $\sin^2$-envelope (40) with length $T_{pulse} = 10\,T_c$ (where $T_c = 2\pi/\omega_c$), and chirp the instantaneous frequency

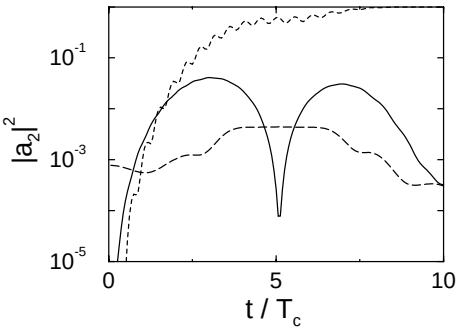

Fig. 9. Dynamics of a chirp over the one-photon resonance of the two-level system (39). The instantaneous frequency of the $\sin^2$-shaped pulse is varied according to equation (66), with $\omega_c = \Delta E/\hbar$ and $\Delta\omega/\omega_c = 0.3$. The maximum field strength is $\mu F_{max}/(\hbar\omega_c) = 0.3$; the pulse length is $T_{pulse} = 10\,(2\pi/\omega_c) \equiv 10\,T_c$. The Schrödinger wave function $|\psi(t)\rangle$ evolving from the initial bare state $|1\rangle$ has been projected onto the bare state $|2\rangle$ (dotted), onto the instantaneous Floquet function $|u_2^{R(t)}(t)\rangle$ (full line), and onto the third-order superadiabatic basis vector $|\psi_2^{(3)}(t)\rangle$ (dashed).

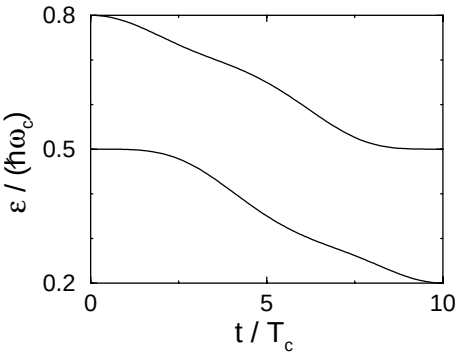

Fig. 10. Quasienergies for the two-level system (39) corresponding to the chirp studied in Figure 9. Note that the quasienergy emerging from the bare state $|1\rangle$ is continuously connected to $|2\rangle$, and *vice versa*.

according to

$$\omega(t) = \omega_c + \Delta\omega\cos(\pi t/T_{pulse}) \tag{66}$$

from above to below the resonance [30]. Figure 9 shows the square of the wave function's projection onto the bare state $|2\rangle$, onto the adiabatic Floquet function $|u_2^{R(t)}(t)\rangle$, and onto the third-order superadiabatic basis vector $|\psi_2^{(3)}(t)\rangle$, for a pulse with $\mu F_{max}/(\hbar\omega_c) = 0.3$ and $\Delta\omega/\omega_c = 0.3$. Despite the pulse's shortness, the chirp effectuates an almost complete population transfer from $|1\rangle$ to $|2\rangle$. This is made possible by the fact that the quasienergy emerging from the initial state $|1\rangle$ is adiabatically connected to the final state $|2\rangle$, as shown in Figure 10. Hence, a chirped laser pulse can induce a "transition without transition": the population can flow to the target state (almost) adiabatically. For the very short pulse considered here, the actual dynamics is more involved: the full line in Figure 9, indicating the transition probability in the adiabatic basis, shows an overshooting of the occupation of $|u_2^{R(t)}(t)\rangle$ by about two orders of magnitude over the actual final non-adiabatic population loss. This is caused by two Landau-Zener-like transitions that occur when the instantaneous quasienergy levels approach each other slightly, comparable to the situation in Figure 8. Unlike the case studied there, the two transition amplitudes do not add constructively, but destructively, as revealed by the transformation to the third-order superadiabatic basis. It is only this transformation which shows the actual magnitude of Landau-Zener-induced losses, and separates them from the loss due to the roughness of the pulse's edges.

5 Sequential ladder climbing versus multiphoton chirp

The ideas illustrated in the previous sections with the help of the model (39) can be exploited in order to develop strategies for efficient population transfer in multilevel systems. As a typical example, we consider the forced Morse oscillator

$$H(t) = \frac{p^2}{2m} + D(1 - e^{-\beta x})^2 + dxF(t)\sin(\phi(t)) \tag{67}$$

with parameters characterizing the vibrations of an HF molecule: $m = 1744.8$, $D = 0.22509$, $\beta = 1.1741$, and $d = 0.3099$ (all data in atomic units [31]). The undriven Morse oscillator then has 24 bound states with energies

$$E_n = \hbar\omega_0\left(n + \frac{1}{2}\right) - \frac{\hbar^2\omega_0^2}{4D}\left(n + \frac{1}{2}\right)^2, \tag{68}$$

where

$$\omega_0 = \sqrt{\frac{2D\beta^2}{m}} \tag{69}$$

is the frequency of small oscillations in the Morse potential. We restrict ourselves to the dynamics in the space spanned by the bound states, thereby excluding continuum effects.

For $F = 0$, the quasienergies $\varepsilon_{(n,m)}$ are related to the energies E_n by

$$\varepsilon_{(n,m)} = E_n + m\hbar\omega. \tag{70}$$

Hence, plotting quasienergies *versus* frequency yields a web of straight lines, as in Figure 11. For $F > 0$ the level crossings seen in this figure, indicating multiphoton resonances, turn into anticrossings, thus providing several alternative routes for adiabatic transfer schemes. For instance, if we start with the vibrational ground state $|0\rangle$ and seek to populate the fifth excited state $|5\rangle$, we may choose to move on the upper envelope of the levels in Figure 11, beginning with a frequency ω_i that is higher than the first transition frequency $(E_1 - E_0)/\hbar$, increase the field amplitude, gradually lower the frequency and successively

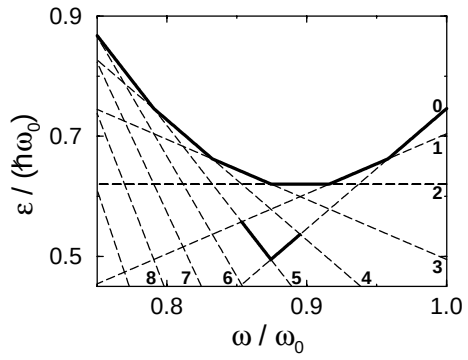

Fig. 11. Quasienergies $\varepsilon_{(n,m)}$ for the HF-Morse oscillator (67), for vanishing amplitude F. The numbers correspond to the vibrational quantum number n; the slope of the lines is determined by m. For $F > 0$ the level crossings turn into anticrossings. In the case of sequential ladder climbing studied in Figure 13, the wave function moves on the upper envelope of these lines (from right to left), whereas a multiphoton chirp exploits an individual anticrossing (with arbitrary chirp direction). The two heavy segments of the lines with $n = 0$ and $n = 5$ indicate the five-photon resonance utilized in Figure 16.

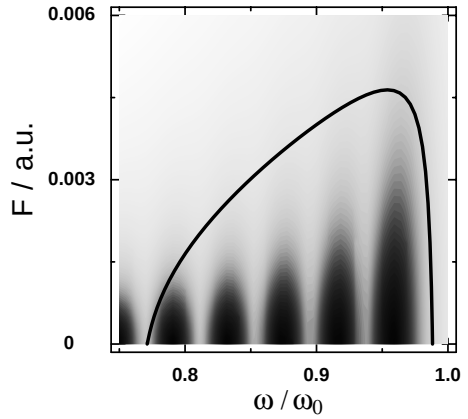

Fig. 12. Greyscale plot encoding the difference $\Delta\varepsilon$ between the instantaneous quasienergy used for successive ladder climbing from $|0\rangle$ to $|5\rangle$ and its nearest neighbor. Black areas correspond to near-degeneracies that are to be circumvented. The heavy line is the path traversed by the pulse (66, 71).

pass the single-photon resonances $\omega = (E_{n+1} - E_n)/\hbar$ for $n = 0, \ldots, 4$ as adiabatically as possible, and finally lower the amplitude back to zero at some frequency $(E_6 - E_5)/\hbar < \omega_f < (E_5 - E_4)/\hbar$. In this way, we successively climb the rungs of the vibrational ladder: on the individual line segments of the upper envelope in Figure 11, the adiabatic Floquet state is closely associated with the respective Morse eigenstate.

While this scenario is well-known in principle [7,32], there is the pertinent question how to design the field amplitude $F(t)$ in order to accomplish the intended population transfer with as little loss as possible. A reasonable guideline for this purpose is varying the pulse parameters such that the difference $\Delta\varepsilon$ between the quasienergy of the transfer state and its nearest neighbor stays roughly

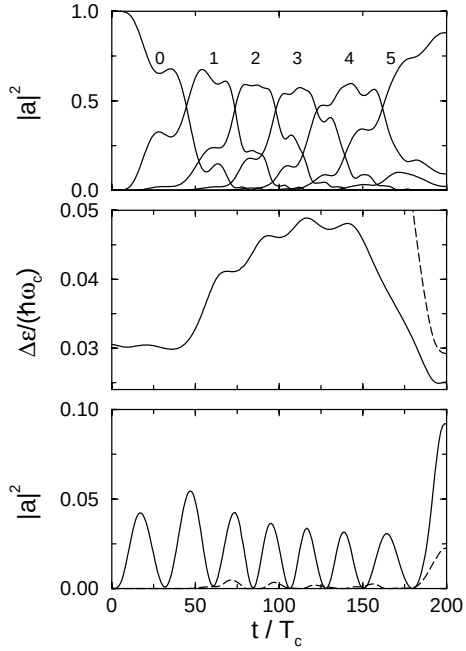

Fig. 13. Upper panel: population of the bare Morse eigenstates during the pulse indicated in Figure 12, with $T_{pulse} = 200\,(2\pi/\omega_c) \equiv 200\,T_c$. One clearly recognizes the climbing of the vibrational ladder from $|0\rangle$ to $|5\rangle$. Middle panel: difference $\Delta\varepsilon$ between the quasienergy of the adiabatically moving Floquet state and its nearest (full line) or next-to-nearest neighbor (dashed) during the pulse. Lower panel: population of the instantaneous Floquet state that is the nearest (full line) or next-to-nearest neighbor (dashed) of the adiabatically moving state, as determined by quasienergy difference. Note that there are seven, not five, Landau-Zener-like overshootings, as corresponding to the precise variation of $\Delta\varepsilon$. Note further that the overall population loss is induced only at the end of the pulse.

constant during the pulse. In Figure 12 we encode this difference in terms of shades of grey; black areas correspond to near-degeneracies that are to be circumvented. Based on this plot, we choose the pulse as indicated by the heavy line, corresponding to a cosine frequency chirp (66) and an envelope parametrized (somewhat arbitrarily) as

$$F(t) = F_0 \left(1 - \frac{at}{T_{pulse}}\right) \frac{4}{\pi^2} \arctan^2 \left(\frac{3\pi^2}{2} \frac{t}{T_{pulse}} \left[1 - \frac{t}{T_{pulse}}\right]\right) \tag{71}$$

for $0 \le t \le T_{pulse}$. We take an asymmetry parameter $a = 0.7$ and set $F_0 = 0.01$ a.u., $\omega_c/\omega_0 = 0.880$, and $\Delta\omega/\omega_0 = 0.109$, so that the frequency is chirped from $\omega_i/\omega_0 = 0.989 = 1.031\,(E_1 - E_0)/(\hbar\omega_0)$ to $\omega_f/\omega_0 = 0.771 = 0.976\,(E_5 - E_4)/(\hbar\omega_0)$, *cf.* Figure 11. The upper panel of Figure 13 then shows the population of the bare Morse eigenstates during such a pulse with length $T_{pulse} = 200\,(2\pi/\omega_c)$; the climbing of the vibrational ladder from $|0\rangle$ to $|5\rangle$ is quite apparent. However, the probability of a transition from the adiabatically moving Floquet state to its nearest neighbor, depicted in the lower

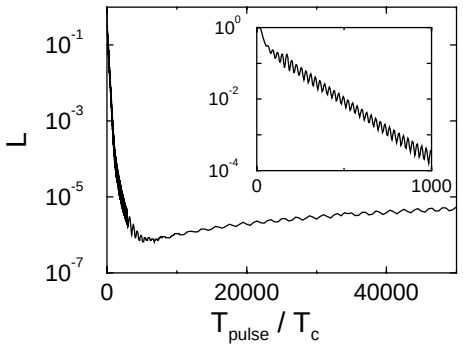

Fig. 14. Total population loss (72) after sequential transfer from the vibrational ground state $|0\rangle$ to the target state $|5\rangle$, induced by chirped pulses (66, 71) with the path indicated in Figure 12. Apart from the variation of the pulse length T_{pulse}, all parameters are the same as in Figure 13. For $T_{pulse} > 2500\,T_c$ the oscillations are not fully resolved.

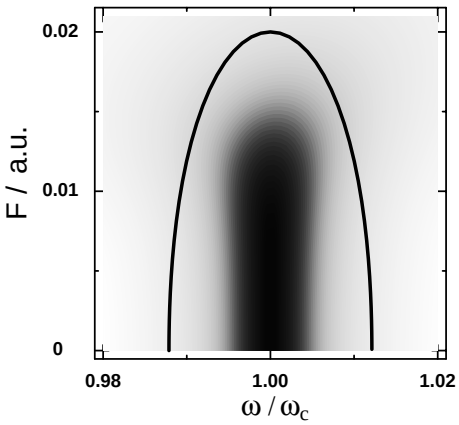

Fig. 15. Greyscale plot visualizing the quasienergy difference $\Delta\varepsilon$ between the adiabatic state and its nearest neighbor (corresponding to the full line in the middle panel of Fig. 16) for the five-photon resonance connecting the bare Morse eigenstates $|0\rangle$ and $|5\rangle$ (*cf.* Fig. 11). The black area marks the near-degeneracy; the heavy line is the path traversed by the pulse discussed in Figure 16.

panel, shows that the naively assumed mechanism – the adiabatic passage through five avoided crossings, corresponding to five single-photon resonances – does not quite match the reality. There are *seven*, not five, Landau-Zener-like overshootings, corresponding to fine details of the behavior of $\Delta\varepsilon$ during the pulse (middle panel). The most interesting detail revealed by the lower panel is that the overall population loss one is left with after the pulse, about 12%, is born only on the very final stage of the pulse. Steering the pulse's path finally between the resonances $\omega = (E_5 - E_4)/\hbar$ and $\omega = (E_6 - E_5)/\hbar$ (*cf.* Fig. 12) requires particular care, since here the quasienergy distances to the next and next-to-nearest neighbors necessarily become quite small. Reduction of the non-adiabatic loss thus requires optimization of the pulse especially at its very end.

For practical purposes, one of the most important issues is the dependence of the transfer efficiency on the duration of the pulse. This is studied in Figure 14, again for the sequential transfer from $|0\rangle$ to $|5\rangle$ and pulses with the same path (66, 71) as before, for pulse durations up to $50\,000\,T_c$ (for orientation: $1000\,T_c$ correspond to 9.16 picoseconds). As seen in the inset, the total population loss

$$L = \sum_{n\neq 5} |a_n(T_{pulse})|^2, \tag{72}$$

i.e., the final population of all vibrational states other than the target state $n = 5$, decreases exponentially with T_{pulse} as long as $T_{pulse} < 1000\,T_c$; we find $L < 1\%$ for $T_{pulse} > 500\,T_c$. This exponential decrease is to be expected if the loss is dominated by a single Landau-Zener-type transition. However, for substantially longer pulses the loss *increases* with T_{pulse}. This increase can be traced to a number of high-order multiphoton resonances which give rise to tiny anticrossings with the quasienergy of the transfer state. As long as the pulse is not too long, these anticrossings are traversed practically diabatically, and therefore do not make themselves felt. For longer pulses, however, their Landau-Zener probabilities become minutely less than unity, thus directing small portions of population into unwanted channels [33]. Hence, there is an optimal pulse length that minimizes the population loss; in the present example, it is about $6000\,T_c$.

As an alternative to the use of successive single-photon resonances, one may also chirp the frequency around a five-photon resonance in order to achieve the transition from $|0\rangle$ to $|5\rangle$ in a single step. This means exploiting the (anti-)crossing of the lines labeled by $n = 0$ and $n = 5$ in Figure 11, so that the total frequency chirp $2\,\Delta\omega$ has to be much smaller than in the previous case. However, there is a trade-off: the greyscale plot of the quasienergy difference between the adiabatic state and its nearest neighbor displayed in Figure 15 indicates that in order to circumvent the devastating near-degeneracy we now need pulse amplitudes that are about 4 times higher than the previous one. Choosing a simple $\sin^2$-envelope (40) with $F_{max} = 0.02$ a.u., and a cosine chirp (66) with central frequency $\omega_c = (E_5 - E_0)/(5\hbar)$ exactly on five-photon resonance, $\Delta\omega/\omega_c = 0.0121$, and $T_{pulse} = 200\,(2\pi/\omega_c)$, we obtain the flow of population displayed in Figure 16. In comparison with its counterpart in Figure 13, the bare state basis now provides hardly any information about the underlying mechanism, since the strong-field Floquet states differ substantially from the unperturbed eigenstates. In contrast, the projection to the adiabatic basis again reveals peaks corresponding to Landau-Zener dynamics, resulting from the close approaches of neighboring quasienergies shown in the middle panel. Interestingly, there are two such peaks, instead of the naively expected one. As opposed to the sequential mechanism considered before, a similar population transfer can also be induced by chirping the frequency from red to blue over the multiphoton resonance (that is, by changing the sign of $\Delta\omega$), since one now has effectively two-level dynamics.

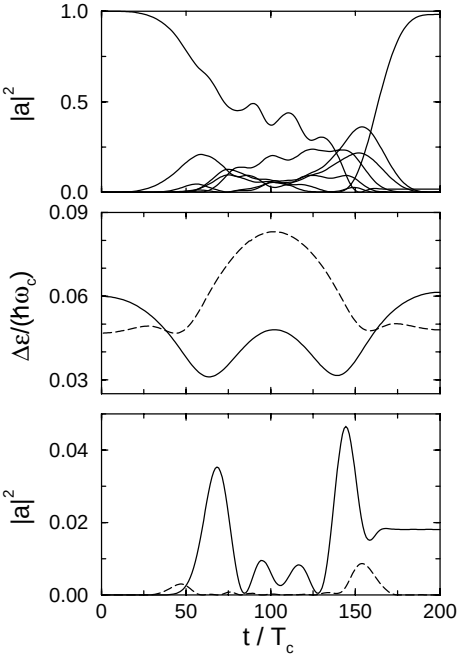

Fig. 16. Population transfer induced by the pulse indicated in Figure 15, for $T_{pulse} = 200\,(2\pi/\omega_c)$. Upper panel: population of the bare Morse eigenstates. Middle panel: difference $\Delta\varepsilon$ between the quasienergy of the adiabatically moving Floquet state and its nearest (full line) or next-to-nearest neighbor (dashed) during the pulse. Lower panel: population of the instantaneous Floquet state that is the nearest (full line) or next-to-nearest neighbor (dashed) of the adiabatically moving state, as determined by quasienergy difference.

6 An application to the STIRAP process

The key principle behind population transfer by frequency chirping is to provide a quasienergy level continuously connecting the initial and the target state, as exemplified in Figure 10. The same idea can also be realized in a different manner, namely, by exposing the system H_0 to *two* laser pulses with different, but fixed carrier frequencies ω_1 and ω_2. Instead of the Hamiltonian (1) one then has

$$H(t) = H_0 + \widehat{\mu}F_1(t)\sin(\omega_1 t) + \widehat{\mu}F_2(t)\sin(\omega_2 t + \vartheta), \quad (73)$$

where ϑ is a phase. If ω_1 and ω_2 are not rationally related, so that $H(t)$ becomes quasiperiodic when the amplitudes F_1 and F_2 are kept fixed, one obtains instantaneous quasienergies in the following way: instead of the Schrödinger wave function $|\psi(t)\rangle$, consider a new function $|\Psi(t_1,t_2)\rangle$ with $|\Psi(t,t)\rangle = |\psi(t)\rangle$. Then the fixed-amplitude Schrödinger equation becomes

$$(\mathcal{H}(t_1,t_2) - i\hbar\partial_{t_1} - i\hbar\partial_{t_2})\,|\Psi(t_1,t_2)\rangle = 0, \quad (74)$$

where the operator

$$\mathcal{H}(t_1,t_2) = H_0 + \widehat{\mu}F_1\sin(\omega_1 t_1) + \widehat{\mu}F_2\sin(\omega_2 t_2 + \vartheta) \quad (75)$$

is periodic in both t_1 and t_2. Hence, the Floquet theorem now suggests solutions of the form

$$|\Psi(t_1,t_2)\rangle = |u(t_1,t_2)\rangle\exp(-i\varepsilon_1 t_1/\hbar - i\varepsilon_2 t_2/\hbar) \quad (76)$$

with doubly periodic functions

$$|u(t_1,t_2)\rangle = |u(t_1+T_1,t_2)\rangle = |u(t_1,t_2+T_2)\rangle \quad (77)$$

for $T_k = 2\pi/\omega_k$, $k = 1,2$. Setting $t_1 = t_2 = t$, this gives Schrödinger wave functions

$$|\psi(t)\rangle = |u(t,t)\rangle\exp(-i\varepsilon t/\hbar) \quad (78)$$

with two-color quasienergies $\varepsilon = \varepsilon_1 + \varepsilon_2$ and quasiperiodic functions $|u(t,t)\rangle$. These states (78) now take over the role of the Floquet states [34]. Proceeding as in Section 2, one can then formulate an adiabatic principle that dictates their response to changes of the amplitudes F_1 and F_2: as in the case of monochromatic driving, the wave functions evolve on "quasienergy surfaces" $\varepsilon^{(F_1,F_2)}$ in a Born-Oppenheimer-like fashion, with deviations from the ideal adiabatic behavior that can be calculated systematically by invoking a suitably extended Hilbert space. There is, however, a mathematical subtlety: the two-color quasienergies ε are defined mod $\hbar\omega_1$ *and* mod $\hbar\omega_2$, so that even an N-level system H_0 gives rise to a dense point spectrum already for vanishing amplitudes. Physically speaking, the resulting abundance of near-degeneracies counteracts adiabatic motion [33], so that substantially more care is needed than in the single-frequency case [35].

A paradigmatic example for population transfer steered by two laser pulses is provided by the STIRAP ("STImulated Raman Adiabatic Passage") mechanism for a three-level Λ-system, in which the initial bare state $|1\rangle$ is connected to the target state $|3\rangle$ only *via* an intermediate state $|2\rangle$ [36–40]. Subjecting this system *first* to a Stokes laser pulse that couples the initially unoccupied states $|2\rangle$ and $|3\rangle$, and *then* to a pump laser pulse coupling the initial state $|1\rangle$ with $|2\rangle$, one gets almost complete population transfer from $|1\rangle$ to $|3\rangle$, provided both pulses have a sufficient overlap in time. Within the rotating wave approximation, this effect finds a transparent explanation: there exists a dressed state (an approximate two-color Floquet state) that adiabatically connects $|1\rangle$ and $3\rangle$, and firing first the Stokes pulse, then the pump pulse amounts to adiabatically shifting the initial to the target state [41–43]. However, the use of the rotating wave approximation in conjunction with adiabatic analysis might not be uncritical, since that approximation implicitly assumes high frequencies, so that the pulses should consist of many optical cycles, which is not necessarily the case.

In this section, we show that the STIRAP principle can be extended to more complex situations even without invoking the rotating wave approximation. The proper way to avoid this approximation is to work with two-color Floquet states [40]; the efficiency of the population transfer in a multilevel system can then be analyzed with tools similar to those developed in Section 3.

We consider again the HF-Morse oscillator (67) of the preceding section, and demonstrate STIRAP-like population transfer from the initial vibrational ground state $|0\rangle$ to the sixth excited state $|6\rangle$ by means of two three-photon resonances: the first pulse has the frequency $\omega_1 = (E_6 - E_3)/(3\hbar)$; the frequency of the second is

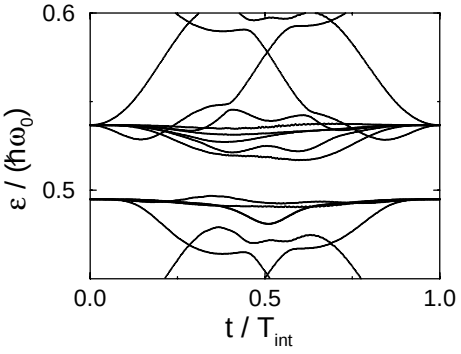

Fig. 17. Instantaneous two-color quasienergies for the HF-Morse oscillator driven by two partially overlapping $\sin^2$-shaped laser pulses of the same length T_{pulse}, with frequencies $\omega_1 = (E_6 - E_3)/(3\hbar)$, $\omega_2 = (E_3 - E_0)/(3\hbar)$, and maximum amplitudes $F_{max,1} = 0.006$ a.u., $F_{max,2} = 0.009$ a.u. The moments of maximum intensity are separated by $\Delta t/T_{pulse} = 0.34$. The quasienergy that permits adiabatic population transfer from the bare Morse eigenstate $|0\rangle$ to $|6\rangle$ is drawn as the heavy line. The total interaction time is $T_{int} = T_{pulse} + \Delta t$. (The tiny wiggles shown by some of the quasienergies are numerical artifacts.)

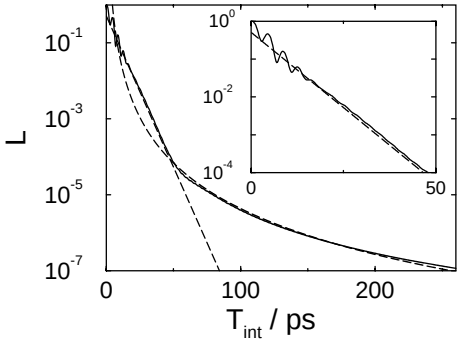

Fig. 18. Total population loss $L = \sum_{n\neq 6} |a(T_{int})|^2$ (full line) for the STIRAP configuration described in Figure 17. For interaction times T_{int} less than 50 picoseconds the loss is well described by an exponential decrease, whereas for longer pulses the loss decreases approximately as T_{int}^{-4}, as indicated by the dashed lines.

$\omega_2 = (E_3 - E_0)/(3\hbar)$; they are applied in the usual counterintuitive order. Both pulses have a $\sin^2$-envelope, and the same length T_{pulse}, with separation Δt between the moments of maximum intensity. The maximum strength of the first pulse is $F_{max,1} = 0.006$ a.u., that of the second is $F_{max,2} = 0.009$ a.u.; the pulse separation is chosen as $\Delta t/T_{pulse} = 0.34$.

Figure 17 shows the most relevant instantaneous quasienergies for this configuration. Because of the particular nature of the unperturbed Morse spectrum (68), and taking into account the $\mathrm{mod}\,\hbar\omega_1$–$\mathrm{mod}\,\hbar\omega_2$-structure of the quasienergy spectrum, initially and finally all quasienergies adopt one of two values that are separated by $\hbar^2\omega_0^2/(2D)$. This multiple degeneracy is removed when the field amplitudes take on non-zero values, and adiabatic transfer from $|0\rangle$ to $|6\rangle$ is made possible because a representative of the quasienergy originating from E_0, indicated by the heavy line, is continuously connected to E_6. Within the usual rotating wave-approach to the STIRAP mechanism in a three-level system, the transfer state is a "dark state", implying that its quasienergy does not depend on the field amplitudes [41]. This changes when the counterrotating components of the fields are taken into account [40]; also in the present multilevel case the quasienergy of the transfer state exhibits a pronounced amplitude-dependence.

The efficiency of this STIRAP process as function of the interaction time $T_{int} = T_{pulse} + \Delta t$, for fixed separation ratio $\Delta t/T_{pulse}$, is depicted in Figure 18; the total population loss is reduced below 1% for interaction times longer than about $2\,750\,(2\pi/\omega_0) \approx 22$ picoseconds. The population loss shows the familiar exponential decrease as long as T_{int} remains below 50 picoseconds, but then vanishes about proportionally to T_{int}^{-4}. This breakdown of the exponential behavior should be contrasted with the breakdown of the Dykhne-Davis-Pechukas formula [18] that has recently been discussed for STIRAP systems [42,43]. The latter stems from the initial and final degeneracy of the quasienergies and emerges even for perfectly smooth pulse envelopes [27], whereas the present T_{int}^{-4}-decay can be traced to the roughness of our $\sin^2$-envelopes. This roughness results, in the language of Section 4, in a non-adiabatic population loss proportional to $(\eta^2)^2 = \eta^4$, with the dimensionless adiabaticity parameter η being proportional to the inverse pulse length.

7 Discussion

The set of the instantaneous Floquet states provides the adiabatic basis for laser-pulsed N-level quantum systems (1). The investigation of the interaction with *short* laser pulses, however, necessitates to leave the adiabatic limit and to estimate transition probabilities. This has been achieved in Section 3 by applying perturbation theory to the Floquet states, after going from the original time-dependent Schrödinger equation (3) to the evolution equation (21) in the extended Hilbert space. From a technical viewpoint, this equation exploits the separation of the "fast" time scale $T = 2\pi/\omega$ and the "slow" time scale characterizing the change of the pulse's envelope or frequency [5,6]. The use of the laser phase ϕ in this equation (21), instead of the time t, is mandatory when the frequency $\omega(t)$ is not constant during the pulse: this is what then allows us to formulate the adiabatic principle for Floquet states in close analogy to its counterpart for adiabatically moving energy eigenstates.

When working in the extended Hilbert space, one can apply standard perturbational techniques; the Fourier modes of a Floquet state are treated like individual states. Although the process of lifting to the extended space is not unique, one always arrives at unique expressions for non-adiabatic transition probabilities, since the ambiguity is removed upon projecting back to the physical space.

This back-projection also reveals a peculiarity of laser-pulsed systems: the occupation probabilities of the instantaneous Floquet states exhibit oscillations that result from the interference of several modes, as expressed by equation (38). It should be emphasized that adiabatic Floquet state perturbation theory, set up in the way described above, cures a shortcoming of the often employed rotating wave approximation. That approximation requires high laser frequencies, and thus presupposes that many laser cycles fall into an interval during which the pulse parameters change significantly, which is at odds with short pulse durations.

The adiabatic basis, adapted to hypothetical pulses with "infinitely slowly" changing parameters, is not satisfactory for monitoring the transition dynamics induced by short pulses. As seen in Figure 8, in the vicinity of a multiphoton resonance there is a temporary excursion of population away from the adiabatic state; the temporary population loss can exceed the actual final non-adiabatic loss by orders of magnitude. In contrast, the use of superadiabatic Floquet bases eliminates such spurious excursions and allows one to keep track of the actual losses. Again working in the extended Hilbert space, these superadiabatic bases have been constructed in Section 4 by transferring Berry's ideas [26] to laser-pulsed systems (1).

Even if one is not interested in the fine details of quantum transition dynamics, but merely wishes to design laser pulses that effectuate population transfer from an initial state to some target state, the Floquet picture yields robust pulse strategies, and physical understanding, by merely inspecting the instantaneous quasienergy spectra, without the need to invoke sophisticated optimization routines. This has been demonstrated in Section 5 by setting up two chirped pulses for a Morse ladder system, obeying the rule to circumvent quasienergetic near-degeneracies. The final example considered in Section 6, a STIRAP-like multiphoton process in a multilevel system, indicates how the investigation of adiabatic Floquet dynamics has to proceed in the two-color case, including the discussion of non-adiabatic losses.

This work was supported by the Deutsche Forschungsgemeinschaft *via* the Schwerpunktprogramm "Zeitabhängige Phänomene und Methoden in Quantensystemen in der Physik und Chemie".

References

1. See, *e.g.*, *Femtosecond Chemistry*, edited by J. Manz, L. Wöste (Verlag Chemie, Weinheim, 1995).
2. J.H. Shirley, Phys. Rev. B **138**, 979 (1965).
3. Ya.B. Zel'dovich, Zh. Eksp. Theor. Fiz. **51**, 1492 (1966); Sov. Phys. JETP **24**, 1006 (1967).
4. R.H. Young, W.J. Deal, J. Math. Phys. **11**, 3298 (1970).
5. H.P. Breuer, M. Holthaus, Z. Phys. D **11**, 1 (1989).
6. H.P. Breuer, M. Holthaus, Phys. Lett. A **140**, 507 (1989).
7. S. Guérin, Phys. Rev. A **56**, 1458 (1997).
8. For a review, see S.-I Chu, Adv. Chem. Phys. **73**, 739 (1989).
9. H. Sambe, Phys. Rev. A **7**, 2203 (1973).
10. J.S. Howland, Math. Ann. **207**, 315 (1974).
11. J.S. Howland, Ind. Uni. Math. J. **28**, 471 (1979).
12. U. Peskin, N. Moiseyev, J. Chem. Phys. **99**, 4590 (1993).
13. M. Born, V. Fock, Z. Phys. **51**, 165 (1928).
14. T. Kato, J. Phys. Soc. Jpn **5**, 435 (1950).
15. A. Messiah, *Quantum Mechanics*, Vol. 2 (North-Holland, Amsterdam, 1962).
16. B.H. Bransden, C.J. Joachain, *Introduction to Quantum Mechanics* (Longman Scientific and Technical, Harlow, 1989).
17. B. Simon, Phys. Rev. Lett. **51**, 2167 (1983).
18. J.P. Davis, P. Pechukas, J. Chem. Phys. **64**, 3129 (1976).
19. J.-T. Hwang, P. Pechukas, J. Chem. Phys. **67**, 4640 (1977).
20. R.B. Dingle, *Asymptotic Expansions: Their Derivation and Interpretation* (Academic Press, New York and London, 1973).
21. L.M. Garrido, F.J. Sancho, Physica **28**, 553 (1962).
22. F.J. Sancho, Proc. Phys. Soc. **89**, 1 (1966).
23. M.V. Berry, Proc. R. Soc. Lond. A **392**, 45 (1984).
24. L.D. Landau, Phys. Z. Sowjetunion **2**, 46 (1932).
25. C. Zener, Proc. R. Soc. Lond. A **137**, 696 (1932).
26. M.V. Berry, Proc. R. Soc. Lond. A **429**, 61 (1990).
27. K. Drese, M. Holthaus, Eur. Phys. J. D **3**, 73 (1998).
28. Yu.N. Demkov, V.N. Ostrovskii, E.A. Solov'ev, Phys. Rev. A **18**, 2089 (1978).
29. A. Joye, C.-E. Pfister, J. Math. Phys. **34**, 454 (1993).
30. For a discussion of chirped pulses in the framework of the rotating wave approximation, see L. Allen, J.H. Eberly, *Optical Resonance and Two-Level Atoms*, Sect. 4.6 (Dover, New York, 1987).
31. R.B. Walker, R.K. Preston, J. Chem. Phys. **67**, 2017 (1977).
32. V.M. Akulin, N.V. Karlov, *Intense Resonant Interactions in Quantum Electronics* (Springer, Berlin, 1992).
33. D.W. Hone, R. Ketzmerick, W. Kohn, Phys. Rev. A **56**, 4045 (1997).
34. T.-S. Ho, S.-I Chu, J. Phys. B **17**, 2101 (1984).
35. P.M. Blekher, H.R. Jauslin, J.L. Lebowitz, J. Stat. Phys. **68**, 271 (1992).
36. C.E. Carroll, F.T. Hioe, Phys. Rev. A **42**, 1522 (1990).
37. B.W. Shore, K. Bergmann, J. Oreg, Z. Phys. D **23**, 33 (1992).
38. S. Schiemann, A. Kuhn, S. Steuerwald, K. Bergmann, Phys. Rev. Lett. **71**, 3637 (1993).
39. A. Kuhn, S. Steuerwald, K. Bergmann, Eur. Phys. J. D **1**, 57 (1998).
40. S. Guérin, H.R. Jauslin, Eur. Phys. J. D **2**, 99 (1998).
41. T.A. Laine, S. Stenholm, Phys. Rev. A **53**, 2501 (1996).
42. N.V. Vitanov, S. Stenholm, Phys. Rev. A **55**, 648 (1997).
43. N.V. Vitanov, S. Stenholm, Opt. Commun. **135**, 394 (1997).